Cancer Research

A2AR Adenosine Signaling Suppresses Natural Killer Cell Maturation in the Tumor Microenvironment

Arabella Young[1,2], Shin Foong Ngiow[1,2,3], Yulong Gao[1,2], Ann-Marie Patch[4], Deborah S. Barkauskas[1], Meriem Messaoudene[5], Gene Lin[6], Jerome D. Coudert[7], Kimberley A. Stannard[1], Laurence Zitvogel[5,8,9], Mariapia A. Degli-Esposti[7], Eric Vivier[10], Nicola Waddell[4], Joel Linden[6], Nicholas D. Huntington[11,12], Fernando Souza-Fonseca-Guimaraes[11,12], and Mark J. Smyth[1,2]

Abstract

Extracellular adenosine is a key immunosuppressive metabolite that restricts activation of cytotoxic lymphocytes and impairs antitumor immune responses. Here, we show that engagement of A2A adenosine receptor (A2AR) acts as a checkpoint that limits the maturation of natural killer (NK) cells. Both global and NK-cell–specific conditional deletion of A2AR enhanced proportions of terminally mature NK cells at homeostasis, following reconstitution, and in the tumor microenvironment. Notably, A2AR-deficient, terminally mature NK cells retained proliferative capacity and exhibited heightened reconstitution in competitive transfer assays. Moreover, targeting A2AR specifically on NK cells also improved tumor control and delayed tumor initiation. Taken together, our results establish A2AR-mediated adenosine signaling as an intrinsic negative regulator of NK-cell maturation and antitumor immune responses. On the basis of these findings, we propose that administering A2AR antagonists concurrently with NK cell–based therapies may heighten therapeutic benefits by augmenting NK cell–mediated antitumor immunity.

Significance: Ablating adenosine signaling is found to promote natural killer cell maturation and antitumor immunity and reduce tumor growth. *Cancer Res; 78(4); 1003–16. ©2017 AACR.*

Introduction

Adenosine is a critical immunosuppressive metabolite, necessary for protecting against an overzealous immune reaction during inflammation and tissue damage (1). In response to hypoxia and extracellular stress, adenosine is generated from ATP by the ectonucleotidase CD39 and CD73 and signals via four G-protein–coupled adenosine receptors (A1, A2A, A2B, and A3; reviewed by ref. 2). The high affinity A2A adenosine receptor (A2AR) is highly expressed on lymphocytes and has been shown to abrogate their activity. In the tumor microenvironment (TME), adenosine signaling via the A2AR prevents an effective antitumor immune response by inhibiting the infiltration and function of $CD8^+$ T and natural killer (NK) cells (3–6). In addition, A2AR signaling has been shown to inhibit macrophage activation (7) and to affect T-lymphocyte proliferation, priming, and cytokine production, leading to polarization in favor of immunosuppressive T regulatory cells (8–10). At homeostasis, A2AR-deficient mice display a reduction of naïve $CD44^{lo}$ $CD4^+$ and $CD8^+$ T cells, suggesting adenosine signaling is critical for T-cell maintenance (11). However, understanding the impact of A2AR signaling on NK cells remains limited to reduced cytotoxicity and cytokine production in response to exogenous adenosine and adenosine analogues *in vitro* (4, 12, 13).

Group 1 innate lymphoid cells include both NK cells and type 1 innate lymphoid cells (ILC1), the latter of which appears to be more restricted to residing in tissues (14). NK cells are innate effector lymphocytes critical for rapid recognition of aberrant transformed or infected cells. Their function is dependent on engagement of activating or inhibitory receptors present on the cell surface, which dictates the release of cytotoxic granules and pro-inflammatory cytokines (14, 15). Functionally distinct NK cell maturation subsets are distinguished by expression of CD11b/CD27/KLRG1 and DNAM-1 in mice (16–18) and CD56/CD16 in humans (19). Deficiency in a number of pathways including IL15 signaling and the transcription factors EOMES,

[1]Immunology in Cancer and Infection Laboratory, QIMR Berghofer Medical Research Institute, Herston, Queensland, Australia. [2]School of Medicine, University of Queensland, Herston, Queensland, Australia. [3]Department of Microbiology and Institute for Immunology, University of Pennsylvania Perelman School of Medicine, Philadelphia, Pennsylvania. [4]Medical Genomics, QIMR Berghofer Medical Research Institute, Herston, Queensland, Australia. [5]INSERM U1015, Gustave Roussy Cancer Campus, Villejuif, France. [6]Division of Developmental Immunology, La Jolla Institute for Allergy and Immunology, and Department of Pharmacology, University of California San Diego, La Jolla, California. [7]Immunology and Virology Program, Centre for Ophthalmology and Visual Science, The University of Western Australia, Crawley, Western Australia, Australia. [8]University Paris-Saclay, Kremlin Bicêtre, France. [9]CIC1428, Gustave Roussy Cancer Campus, Villejuif, France. [10]Centre d'Immunologie de Marseille-Luminy, Aix Marseille Université, Inserm, CNRS, France. [11]Molecular Immunology Division, The Walter and Eliza Hall Institute of Medical Research, Department of Medical Biology, The University of Melbourne, Parkville, Victoria, Australia. [12]Faculty of Medicine, Dentistry and Health Sciences, University of Melbourne, Melbourne, Victoria, Australia.

Note: Supplementary data for this article are available at Cancer Research Online (http://cancerres.aacrjournals.org/).

Corresponding Author: Mark J. Smyth, QIMR Berghofer Medical Research Institute, 300 Herston Road, Herston 4006, Australia. Phone: 61-7-3845-3957; Fax: 61-7-3362-0111; E-mail: mark.smyth@qimrberghofer.edu.au

doi: 10.1158/0008-5472.CAN-17-2826

GATA-3, AIOLOS, ZEB2, and T-BET prevents the development of mature NK cells (20–24). However, regulatory pathways that drive NK cell maturation remain poorly defined. Recently, accumulation of functionally mature NK cells was identified in mice with FOXO1-deficient NK cells (25). Because of their ability to generate a fast-acting, antigen-independent host immune response, NK cells are being increasingly considered for their therapeutic potential. Identifying pathways that enhance the accumulation of functionally mature NK cells is of great interest.

Here, we show that deficiency in A2AR signaling enhances NK-cell maturation at homeostasis, with terminally mature NK cells displaying increased function and antitumor immunity. Currently, A2AR antagonists are undergoing clinical trials for their safety and efficacy in solid tumors either alone or in combination with other immunotherapies (NCT02655822 and NCT02403193). Based on our findings, the use of A2AR antagonists as an adjuvant therapy to potentiate NK cell–based immunotherapy efficacy should be considered.

Materials and Methods

Mice

C57BL/6 wild-type (WT) and B6.SJL-PTPRCA (PTPRCA; CD45.1$^+$) mice were purchased from Walter and Eliza Hall Institute for Medical Research or bred in-house at the QIMR Berghofer Medical Research Institute. C57BL/6 A2AR-deficient (A2AR.KO) mice (6) and Rag2$^{-/-}$IL2r$\gamma^{-/-}$ (26) were as previously described. Floxed A2AR mice (A2AR$^{fl/fl}$; ref. 11) were crossed with *Ncr1*^{iCre} (27) to generate *Ncr1*^{iCre}A2AR$^{fl/fl}$ (A2AR$^{\Delta NK}$). *Ncr1*^{WT}A2AR$^{fl/fl}$ (A2AR^{WT}), *Ncr1*^{iCre}A2AR$^{WT/WT}$ (WT$^{\Delta NK}$), and *Ncr1*^{iCre}R26R^{eYFP} (Rosa-YFP$^{\Delta NK}$) were used as controls. WT and all gene-targeted strains were used between the ages of 8 and 25 weeks. Groups of 4 to 25 mice per experiment were used for experimental tumor assays and competitive reconstitutions, to ensure adequate power to detect biological differences. All experiments were approved by the QIMR Berghofer Medical Research Institute Animal Ethics Committee.

Tumor cell lines

The C57BL/6 SM1WT1 melanoma cells were derived from the spontaneously arising BRAF^{V600E} SM1 cell line originally isolated from a transgenic mouse, and were grown as described (28, 29). Briefly, SM1WT1 cells were grown in RPMI1640 (Gibco) supplemented with 10% FCS, 1% Glutamax (Gibco), and 1% penicillin/streptomycin (Gibco) and maintained at 5% CO_2. All cell lines were routinely tested negative for Mycoplasma using the Lonza MycoAlert Mycoplasma Detection Kit, but cell line authentication was not routinely performed.

Antibodies and reagents

5′-(N-Ethylcarboxamido)adenosine (NECA), SCH58261 (A2ARi), and PSB1115 (A2BRi) were purchased from Sigma and used at 1 μmol/L *in vitro*. NECA was administered *in vivo* by intraperitoneal injection at 0.05 mg/kg by the schedule indicated. Purified control Ig (clone 1-1) and anti-asialoGM1 (asGM1) were given intraperitoneally at 100 μg on day −1, 0, 7, and 14 of experimental tumor assays.

In vivo tumor models

For primary tumor growth experiments, SM1WT1 (10^6) cells were injected subcutaneously into mice in a volume of 100 μL (day 0). Tumor growth measured using digital calipers and tumor sizes represented as mean ± SEM. As indicated, tumors were excised and mass (in mg) measured for individual mice. For methylcholanthrene (MCA) carcinogen-induced fibrosarcoma, male mice of the indicated genotypes were injected subcutaneously with 300 μg MCA (Sigma) in 100 μL dissolved in sterile corn oil. Fibrosarcoma development was monitored for over 200 days. The percentage of tumor-free mice was determined, tumors were recorded following a minimum of two consecutive measurements of increasing growth greater than 10 mm^2.

Flow cytometry analysis

Tumors, peripheral tissues (spleen, BM, lung, liver), and blood were harvested from mice of various genotypes as indicated. Tumors and lungs were minced and digested with 1 mg/mL collagenase IV (Worthington Biochemical) and 0.02 mg/mL DNase I (Roche), and homogenized to prepare single cell suspensions. Spleens were homogenized and red blood cells (RBC) lysed in preparation for flow cytometry. Similarly, RBCs from peripheral blood samples were lysed twice in preparation for flow cytometry. Digested MCA tumor suspensions and homogenized liver samples, were enriched for lymphocytes using 37.5% Percoll solution (GE Healthcare) and centrifugation at 690 × *g* for 12 minutes. For surface staining, tumor-infiltrating leukocytes (TIL) or immune cell suspensions were stained with monoclonal antibodies against CD45.2 (104), CD45.1 (A20), CD4 (RM4-5), CD8α (53-6.7), TCRβ (H57-597), CD3ε (145-2C11), CD19 (6D5), Gr-1 (RB6-8C5), F4/80 (BM8), TCRγ/δ (GL3), NK1.1 (PK136), NKp46 (29A1.4), CD49a (Ha31/8), CD49b (DX5), CD11b (M1/70), CD27 (LG.7F9), KLRG1 (2F1/KLRG1), CD73 (TY/23), CD39 (24DMS1), Ly49C/I (5E6), c-kit (2B8), CD3 (OKT3), CD56 (HCD56), and respective isotype antibodies (eBioscience, BD Biosciences, Biolegend) in the presence of anti-CD16/32 (2.4G2). 7AAD or Zombie Aqua (Biolegend) was used to exclude dead cells. Cell number was calculated using BD Liquid Counting Beads (BD Biosciences) with the count per organ or per ml of blood shown. Cells were acquired on the BD LSR II Fortessa (BD Biosciences) and analysis was carried out using FlowJo (Tree Star).

Cell sorting

Mouse NK cells (7AAD$^-$, TCRβ$^-$, NK1.1$^+$, NKp46$^+$) were sorted as a whole population or divided into maturation subsets based on CD11b and CD27 expression. Prior to antibody staining and cell sorting, NK cells were enriched using the NK Cell Isolation Kit II and autoMACS Pro Separator (both Miltenyi Biotec). CD4$^+$ and CD8$^+$ T cells were stained (7AAD$^-$, TCRβ$^+$, CD4$^+$, or CD8$^+$, respectively) and sorted from the autoMACS depleted fraction. For human NK cells, peripheral blood mononuclear cells (PBMC) were derived and cryopreserved from blood donor buffy coats, following enrichment by ficol density gradient centrifugation. Further purification of cryopreserved PBMCs was performed using the human NK Cell Isolation Kit and autoMACS Pro Separator (both Miltenyi Biotec). Following, human NK cells (7AAD$^-$, CD3$^-$, CD56$^+$) were sorted.

Human samples

For healthy human A2AR staining by flow cytometry, PBMCs were obtained from volunteers with the approval and consent of the La Jolla Institute Institutional Review Board (protocol

#VD-057). RBCs were lysed (Biolegend) and remaining cells were stained with cell surface markers against CD19 (SJ25-C1), CD3 (UCHT1), CD4 (RPA-T4), CD56 (HCD56), NKp46 (9E2; Life Technologies, BD Biosciences, eBioscience, Biolegend) with Live/Dead fixable viability stain (Life Technologies). Cells were fixed (BD Biosciences) and intracellular staining with a monoclonal antibody against A2AR (7F6-G5-A2; ref. 30) was performed.

The study of gastrointestinal stromal tumors (GIST) patient specimens (TILs and PBMCs) was undertaken in accordance with the Declaration of Helsinki and approved by the Ethic Committee (2007-A00923-50) and all patients provided written informed consent for participation as previously described (31). Antibodies targeting the following human epitopes were purchased from Biolegend, CD3 (OKT3), CD56 (N901), eBiosciences CD73 (AD2), CD39 (eBioA1), and BD Biosciences CD14 (M5E2) CD19 (HIB19). Dead cells were excluded using the Live/Dead Fixable Yellow Dead Cell Stain Kit (Life Technologies). Cell samples were acquired on a BD FACS Canto II flow cytometer and data analyzed with BD FACSDiva software.

In vitro NK-cell culture

Sorted mouse splenic NK cells were labeled with Cell Trace Violet (CTV; Invitrogen) prior to being seeded in equivalent numbers between genotypes or treatment groups within the same experiment in 96-well U bottom plates (Greiner Bio-One) containing RPMI1640 supplemented with 10% FCS, 1% non-essential amino acids (Gibco), 1% sodium pyruvate (Gibco), 10 mmol/L HEPES, 1% GlutaMAX, 0.1% 2-mercaptoethanol (Gibco), 1% penicillin/streptomycin in the presence of rIL15/IL15Rα complex (10 ng/mL; eBioscience) at 5% CO_2 for 3 to 4 days. Human NK cells were cultivated in RPMI1640 supplemented media (described above) in the presence of IL2 (50 U/mL) for 6 days.

Quantitative real-time PCR

RNA was isolated from sorted splenic NK cells, $CD4^+$ and $CD8^+$ T cells following the manufacturer's instructions for RNAzol (Sigma). cDNA synthesis was performed in a 20 μL reaction containing 500 μmol/L dNTP mix, 500 nmol/L OligodT, 20 U of Ribosafe RNase Inhibitor, and 200 U of Tetro Reverse Transcriptase (Bioline) at 42°C for 50 minutes. Reactions were heat inactivated at 85°C for 5 minutes, cDNA product was diluted to 10 ng/mL, and 2 μL of cDNA was subjected to 10 μL real-time PCR reaction using SensiFAST SYBR Lo-ROX Kit (Bioline) and primers (IDT) on Applied Biosystems ViiA 7 Real-Time PCR system. Relative expression of the gene of interest was compared with the housekeeping gene *HPRT* using the primer sets detailed in Supplementary Methods.

NK-cell transfer assays

Sorted splenic NK cells as specified from the indicated genotypes were mixed at a 50:50 ratio of 10^5 cells each and were intravenously injected in to $Rag2^{-/-}IL2r\gamma^{-/-}$ recipients. Flow cytometry was used to assess reconstitution from serial bleeds and at endpoint peripheral lymphoid tissues of recipients.

Bone marrow chimeras

Recipient PTPRCA mice received two doses of 550 cGy total body irradiation, separated by 3 hours to minimize gastrointestinal toxicity. Following, WT and A2AR.KO or $A2AR^{\Delta NK}$ and $Rosa\text{-}YFP^{\Delta NK}$ donor bone marrow was mixed at a 50:50 ratio and injected intravenously on day 0. Reconstitution was assessed by flow cytometry from serial bleeds or at endpoint in peripheral lymphoid tissues of recipients.

RNA-seq

Sorted splenic NK-cell populations differentiated on CD11b and CD27 expression were acquired. RNA was isolated using the RNeasy Micro Kit (Qiagen). Sample quality control (RIN > 8.0), library preparation and sequencing were performed at AGRF using the Illumina HiSeq2000 platform receiving 20 million 50 bp single-end reads per sample. Sequence reads were aligned to the *Mus musculus* GRCm38 (MM10) using the gene, transcript, and exon features model of Ensembl (release 75) using STAR (version 2.5.2a; ref. 32). Gene expression was estimated using RSEM (version 1.2.30; ref. 33). Protein coding genes with <5 counts per million in fewer than two samples were removed and Trimmed mean of M-values (TMM) normalization and differential gene expression analysis performed using the edgeR package (34) and has been deposited in the European Nucleotide Archive (accession no.: PRJEB22631). Differentially expressed genes had a fold change exceeding 1.5 and a multiple-test corrected (Benjamini–Hochberg procedure) false discovery rate of <0.05. RNA-seq performed on CLP, NKP, ILC1s, and NK-cell populations from bone marrow, spleen, and liver was previously described (21, 23, 35, 36).

Statistical analysis

Statistical analyses were carried out using GraphPad Prism software. Significant differences were determined by log-rank (Mantel–Cox) *t* test, Mann–Whitney *U* test, unpaired, and paired *t* test as specified. Values of $P < 0.05$ were considered significant.

Results

A2AR-deficient mice accumulate terminally mature NK cells

To investigate the role of adenosine signaling on mouse NK cells, we first determined the gene expression of all four adenosine receptors during NK-cell development. High A2AR mRNA expression was previously identified on splenic NK cells, compared to T-cell subsets and tumor cells (37). Using RNA-seq data from isolated bone marrow (BM) common lymphoid progenitor (CLP), NK-cell progenitor (NKP), and splenic populations at different stages of NK cell maturity (defined by CD11b, CD27 and KLRG1), we found that *ADORA2A* (encoding the A2AR) was the predominant adenosine receptor encoding gene expressed (Fig. 1A). Next, we assessed whether A2AR-deficient mice (A2AR.KO) displayed alterations to NK-cell proportions and numbers. Consistent with previous reports, NK cells were equivalent between WT and A2AR.KO mice within spleen, blood, and lung, with a minor reduction identified in the BM (Fig. 1B; refs. 6, 11). Liver-derived ILC1s (defined as $CD49a^+$) and conventional NK (cNK) cells ($CD49b^+$) also displayed high *ADORA2A* (A2AR) gene expression compared to other adenosine receptors (Supplementary Fig. S1A). Equivalent proportions and numbers of these cell types were identified in WT and A2AR.KO mice at homeostasis (Supplementary Fig. S1B and S1C), although, ILC1s preferentially expressed adenosinergic pathway markers, CD73 and CD39 (Supplementary Fig. S1D). Notably, A2AR.KO mice displayed an increased proportion of terminally mature NK cells ($CD11b^+CD27^-$) and a corresponding reduced fraction of less mature NK cells ($CD11b^+CD27^+$) within the periphery (Fig. 1C).

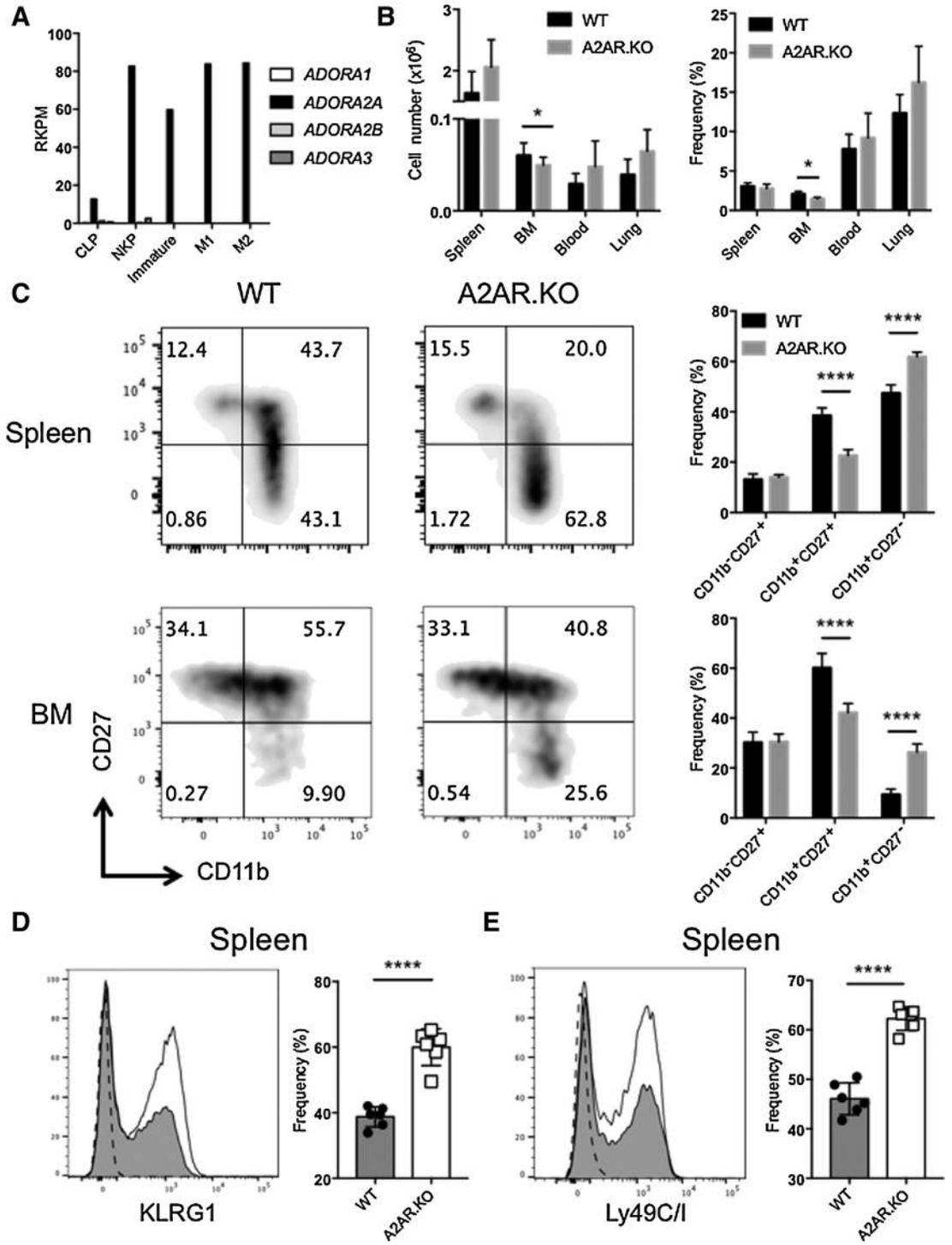

Figure 1.

A2AR adenosine signaling limits NK-cell maturation. **A,** RNA was isolated from sorted populations from BM (common lymphoid progenitor, CLP; NK progenitor, NKP) and spleen (immature, M1, and M2 NK-cell subsets) and subjected to RNA-seq analysis. Reads per kilobase per million (RPKM) mapped to the indicated genes for the cell populations are shown. RNA-seq data have been previously reported (21, 23, 35, 36). **B,** Frequency and enumeration of NK cells ($TCR\beta^-NK1.1^+NKp46^+$ of $CD45.2^+$ viable cells) from C57BL/6 WT or A2AR.KO mice in the indicated organs (spleen, BM, blood, lung). **C,** Flow cytometric analysis and proportions of NK-cell maturation subsets based on CD11b and CD27 expression in the indicated organs (spleen, BM). **D** and **E,** Flow cytometric analysis and proportions of $KLRG1^+$ (**D**) and $Ly49C/I^+$ (**E**) expressing populations from splenic NK cells. Representative histogram comparing expression from individual A2AR.KO (unshaded histogram) and WT (shaded histogram) mice, isotype control (dashed line). Results are presented as mean ± SD from one representative experiment of four to six mice per group. *, $P < 0.05$; ***, $P < 0.001$; ****, $P < 0.0001$ determined by unpaired t test.

Similarly, an accumulation of NK cells expressing the maturation markers KLRG1 and Ly49C/I was also identified (Fig. 1D and E). This may indicate that A2AR adenosine signaling negatively regulates the transition from $CD11b^+CD27^+$ to terminally mature $CD11b^+CD27^-$ NK cells, but not early-stage developmental processes, at homeostasis.

A2AR adenosine signaling limits NK-cell proliferation

Next, we wanted to assess whether NK-cell proliferation was altered in response to adenosine signaling. Sorted NK cells ($TCR\beta^-NK1.1^+NKp46^+$) stimulated *in vitro* with rIL-15/IL-15Rα displayed reduced proliferation in response to the non-selective adenosine agonist NECA (Fig. 2A). A2AR, but not A2BR, antagonism or A2AR gene-deficiency rescued NK-cell proliferative capacity inhibited by NECA (Fig. 2A and B). We then compared the proliferation of splenic A2AR-deficient ($CD45.2^+$) NK cells in competition at a 50:50 ratio with congenic PTPRCA WT ($CD45.1^+$) NK cells. Interestingly, when transferred into a $Rag2^{-/-}IL2r\gamma^{-/-}$ recipient, A2AR-deficient NK cells displayed greater reconstitution than PTPRCA WT NK cells (Fig. 2C and D). As A2AR.KO mice possess higher proportions of terminally mature NK cells ($CD11b^+CD27^-$), which display limited proliferation (16), it was expected that their proliferative capacity would be diminished, but this was not the case.

Next we assessed the competitive proliferation of BM-derived NK cells from PTPRCA WT ($CD45.1^+$) or A2AR.KO ($CD45.2^+$) mice transferred at a 50:50 ratio (Supplementary Fig. S2). Following 14 weeks of reconstitution, A2AR.KO NK cells displayed enhanced proportions within the periphery (Fig. 2E). As seen at homeostasis, phenotypically A2AR-deficient NK cells also displayed a higher proportion of terminally mature NK cells, defined by $CD11b^+CD27^-$, $KLRG1^+$, and $Ly49C/I^+$, than PTPRCA NK cells within the same recipient (Fig. 2F–H).

Together, this indicates that A2AR adenosine signaling impacts NK-cell proliferation and limits NK-cell maturation at both homeostasis and within a competitive setting.

Terminally mature A2AR-deficient NK cells retain proliferative capacity

Next, we determined differences in the transcriptional regulation of $CD11b^+CD27^-$ NK cells from either C57BL/6 WT or A2AR.KO mice. Notably, $CD11b^+CD27^-$ NK cells from A2AR.KO mice displayed differential expression of genes related to cell survival and replication, cell signaling and differentiation, and metabolic processes (Fig. 3A). Consistent with these features, in response to rIL15/IL15Rα stimulation, $CD11b^+CD27^-$ A2AR.KO NK cells continue to proliferate (Fig. 3B). Additionally, when competitively transferred at a 50:50 ratio into $Rag2^{-/-}IL2r\gamma^{-/-}$ recipients, A2AR.KO $CD11b^+CD27^-$ NK cells displayed greater reconstitution in comparison to PTPRCA WT $CD11b^+CD27^-$ NK cells (Fig. 3C).

NK-cell–specific deletion of the A2AR maintains enhanced NK-cell maturation and competitive reconstitution

We next generated a NK-cell–specific A2AR-deficient mouse by crossing the $Ncr1^{iCre}$ ($^{\Delta NK}$) mice in which the gene encoding the improved Cre (iCre) recombinase was inserted into the *Nkp46* locus (27) with A2AR floxed mice (11). We first validated that NK cells isolated from $A2AR^{\Delta NK}$ mice displayed reduced *ADORA2A* gene expression (Fig. 4A). In comparison to littermate controls, mice with A2AR-deficient NK cells ($A2AR^{\Delta NK}$) displayed a mild, but significant, decrease in cell numbers and proportions of NK cells within the spleen and BM, but not blood and lung (Fig. 4B). We next looked at whether alterations to NK cell maturation were maintained when the A2AR-deficiency was exclusive to NK cells. Notably, in comparison to mice carrying either cre ($WT^{\Delta NK}$) or floxed ($A2AR^{WT}$) alleles alone, $A2AR^{\Delta NK}$ mice displayed significantly increased proportions of maturation markers such as $Ly49C/I^+$, $KLRG1^+$ and $CD11b^+CD27^-$ NK cell subsets and decreased $c\text{-}kit^+$ NK cells (Fig. 4C). We examined c-kit expression as it is an alternate maturation marker downregulated in our RNA-seq analysis; however, it has also previously been shown to relate to a proportion of NK cells that show an inability to control tumor (38).

We next compared the reconstitution of BM-derived NK cells from $A2AR^{\Delta NK}$ or $Ncr1^{iCre}$ $R26R^{eYFP}$ ($Rosa\text{-}YFP^{\Delta NK}$) control mice transferred at a 50:50 ratio into a PTPRCA ($CD45.1^+$) recipient (Supplementary Fig. S3). Following 14 weeks of reconstitution, NK cells from $A2AR^{\Delta NK}$ mice displayed significantly higher reconstitution within multiple organs from recipients (Fig. 4D). In addition, reconstituted NK cells from $A2AR^{\Delta NK}$ mice retained a higher proportion of mature NK cells ($KLRG1^+$, $CD11b^+CD27^-$) compared to the competing $Rosa\text{-}YFP^{\Delta NK}$ NK cells from the same recipient (Fig. 4E).

Collectively these data indicated that the effect of global loss of host A2AR on NK-cell terminal differentiation and proliferation was intrinsic to NK cells.

A2AR-deficient NK cells improve tumor control and reduce tumor initiation

As adenosine is a critical immunosuppressive metabolite increased within the tumor microenvironment, we wanted to assess whether adenosine signaling by the A2AR on NK cells was able to impact tumor control. To assess this we utilized the transplantable SM1WT1 BRAF-mutant melanoma, for which A2AR-deficient mice display improved tumor control (6). SM1WT1-tumor-bearing mice display high levels of NK-cell infiltration (~10%) equivalent to other lymphocyte populations such as $CD4^+$ and $CD8^+$ T cells during early phases of tumor growth (6). Here, we identified that $A2AR^{\Delta NK}$ mice displayed reduced tumor growth and this was NK-cell dependent (Fig. 5A and B). Interrogating TILs at endpoint revealed no changes to proportions of lymphocytes; however, a significant reduction in $CD11b^+$ $Gr\text{-}1^{hi}$ myeloid cells was observed (Supplementary Fig. S4A). It is difficult to assess whether this a direct effect of A2AR-deficiency on NK cells or due to the reduction in tumor size that may lead to a less suppressive tumor microenvironment. In comparison to splenic NK cells, tumor-infiltrating NK cells have increased CD73 expression, and this was not altered by A2AR-deficiency (Fig. 5C; Supplementary Fig. S4B). In contrast, CD39 was increased within the tumor microenvironment of $A2AR^{\Delta NK}$ mice alongside $CD11b^+CD27^-$ NK cells, with a reduction in both $CD11b^+CD27^+$ and $c\text{-}kit^+$ expressing NK-cell populations (Fig. 5D and E).

Using the *de novo* carcinogenesis MCA-induced fibrosarcoma model, we assessed whether tumor initiation was impeded in $A2AR^{\Delta NK}$ mice. Previously, NK cells have been shown to control MCA-induced fibrosarcoma development (39). Preventing host A2AR adenosine signaling has also been shown to limit tumor development (6, 40). Interestingly, targeting the A2AR specifically on NK cells provided protection against MCA-induced

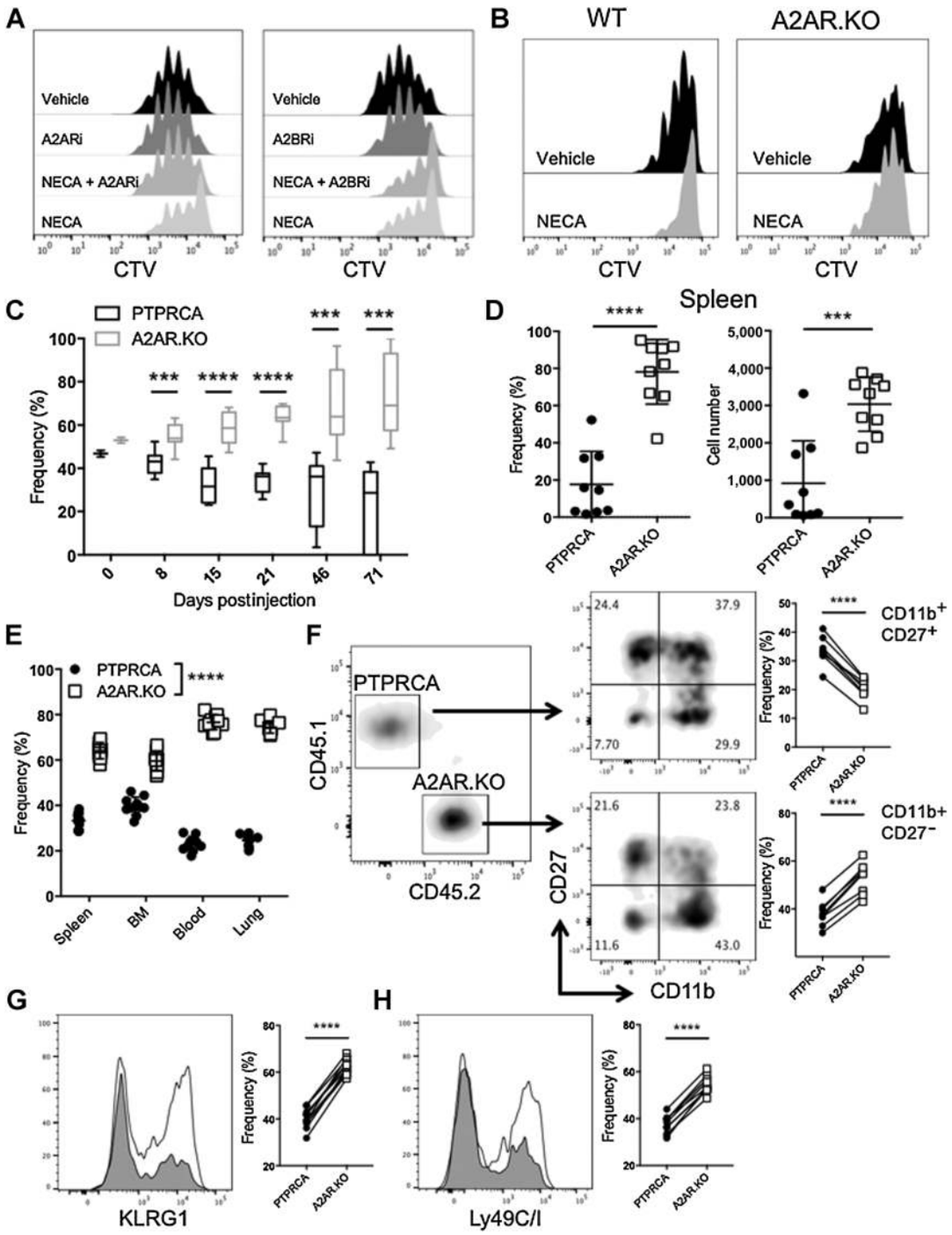

Figure 2.

Adenosine inhibits NK-cell proliferation. **A,** Sorted WT splenic NK cells labeled with CTV were cultured for 4 days *in vitro* in rIL15/IL15Rα (10 ng/mL) in the presence of vehicle (DMSO), A2ARi (SCH58261, 1 μmol/L), A2BRi (PSB1115, 1 μmol/L), or NECA (1 μmol/L) as specified. **B,** C57BL/6 WT or A2AR.KO-sorted splenic NK cells labeled with CTV were cultured for 4 days *in vitro* in rIL15/IL15Rα (10 ng/mL) in the presence of vehicle (DMSO) or NECA (1 μmol/L). **C,** Sorted splenic PTPRCA ($CD45.1^+$) or A2AR.KO ($CD45.2^+$) NK cells were mixed at a 50:50 ratio and injected into $Rag2^{-/-}IL2r\gamma^{-/-}$ recipients. Proportions of reconstituted NK cells in the blood were assessed by flow cytometry at the indicated time-points and are presented as median ± SD. **D,** As in **C**, the proportion and number of reconstituted NK cells in the spleen was assessed by flow cytometry after 14 weeks. **E,** Competitive bone marrow chimeras at a 50:50 ratio of PTPRCA ($CD45.1^+$) and A2AR.KO ($CD45.2^+$) donor NK cells were injected into PTPRCA recipients. Proportions of reconstituted NK cells were assessed by flow cytometry after 14 weeks in the indicated organs (spleen, BM, blood, lung). Comparison of statistical significance between PTPRCA and A2AR.KO reconstitution in each organ is shown. **F–H,** As in **E**, flow cytometric analysis of maturation markers CD11b and CD27 (**F**), KLRG1 (**G**), and Ly49C/I (**H**) expression from donor PTPRCA ($CD45.1^+$) and A2AR.KO ($CD45.2^+$) NK cells were compared from the same recipient. Results shown are from one representative biological replicate (**A** and **B**), two representative donor pairs reconstituting nine recipients (**C** and **D**), and two representative donor pairs reconstituting seven to nine recipients (**E–H**). Data are presented as mean ± SD unless indicated. ***, $P < 0.001$; ****, $P < 0.0001$ determined by unpaired *t* test (**C–E**) and paired *t* test (**F–H**) from donor NK cells isolated from a shared recipient.

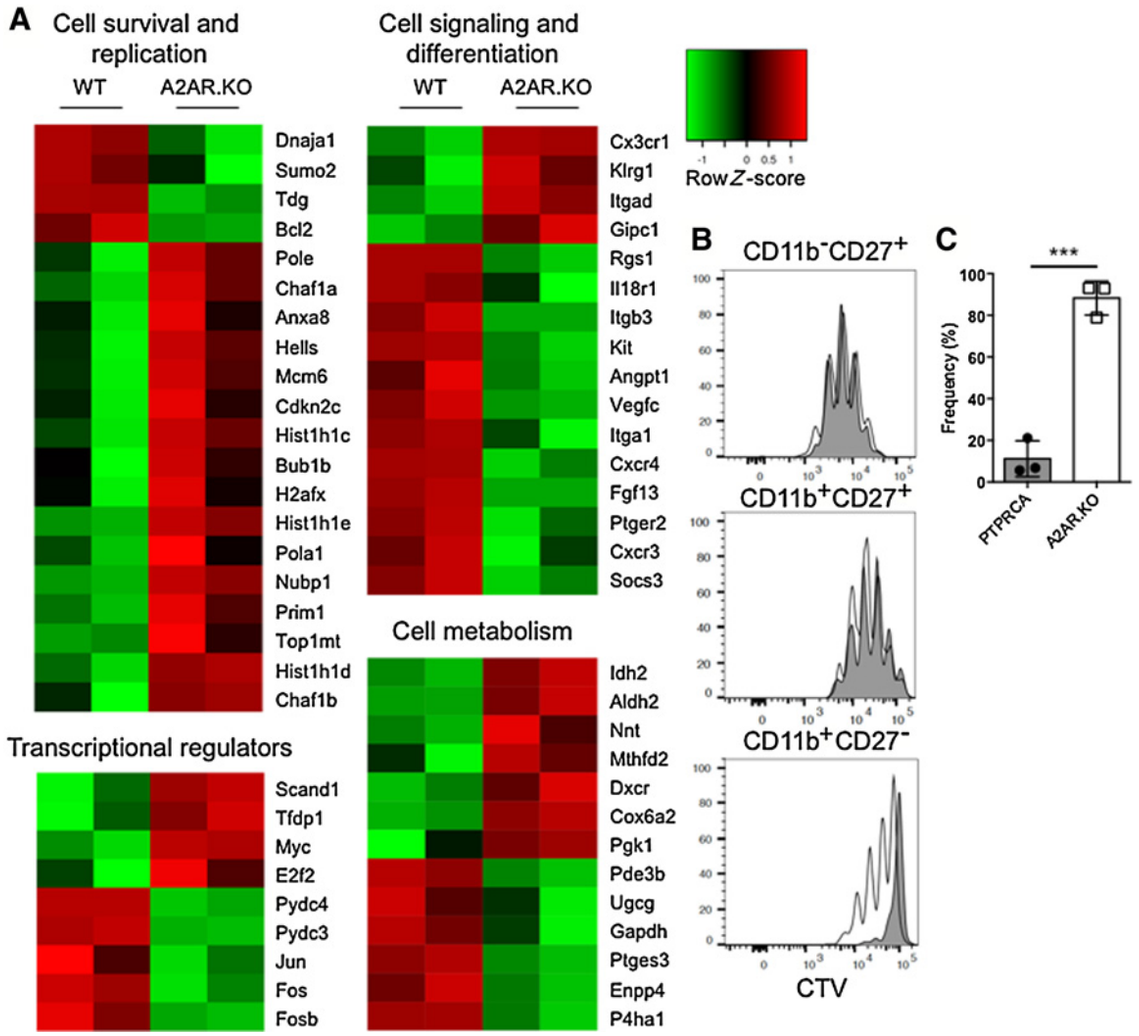

Figure 3.

Terminally mature A2AR-deficient NK cells maintain improved DNA replication and proliferative capacity. **A,** RNA was isolated from CD11b^{+}CD27^{-} splenic NK cells from C57BL/6 WT or A2AR.KO mice and RNA-seq performed. Heatmaps of differentially expressed candidate genes within different biological functional groups as compared between WT and A2AR.KO mice for CD11b^{+}CD27^{-} NK cells. **B,** Maturation subsets isolated from C57BL/6 wild type (shaded histogram) and A2AR.KO (unshaded histogram) mice were stimulated with rIL15/IL15Rα (10 ng/mL) and profileration after 4 days assessed by flow cytometry. **C,** Sorted splenic CD11b^{+}CD27^{-} NK cells isolated from PTPRCA (CD45.1^{+}) and A2AR.KO (CD45.2^{+}) mice were mixed at a 50:50 ratio and injected into Rag2$^{-/-}$IL2rγ$^{-/-}$ recipients. Reconstitution was assessed by flow cytometry after 14 weeks. Results presented as mean ± SD. ***, $P < 0.001$ determined by unpaired t test.

tumorigenesis (Fig. 5F). Similarly to SM1WT1 tumors, interrogating MCA fibrosarcoma-infiltrating leukocytes also revealed decreased c-kit and increased CD39 expression on NK cells isolated from A2AR$^{\Delta NK}$ mice (Fig. 5G).

The findings indicate that preventing A2AR adenosine signaling specifically in NK cells provides protection against tumor initiation and development. Consistent with homeostasis, A2AR-deficient NK cells also display enhanced maturation and differentiation within the tumor microenvironment.

Exogenous adenosine modulates maturation and adenosinergic pathway mediators in NK cells

As loss of A2AR adenosine signaling enhanced NK-cell maturation, we next determined whether exogenous adenosine elicited opposing effects. Following administration of NECA to mice, the proportions of mature NK cells, defined as CD11b^{+}KLRG1^{+}, were significantly reduced, with a reciprocal increase in CD11b^{+}KLRG1^{-} NK cells (Fig. 6A). These changes further highlight the intrinsic role of A2AR adenosine signaling as a negative regulator of NK-cell maturation. In addition, NECA administration also modulated the expression of key enzymes within the adenosinergic pathway, resulting in decreased CD39 and increased CD73 expression on NK cells (Fig. 6B and C). Notably, when we treated A2AR$^{\Delta NK}$ mice with NECA changes to maturation markers were not observed, indicating that these alterations were directly due to engagement of the A2AR on NK cells (Fig. 6D and E).

As CD39 expression was altered in both A2AR-deficient NK cells from the tumor microenvironment and in response to adenosine, we wanted to further interrogate which NK-cell subsets

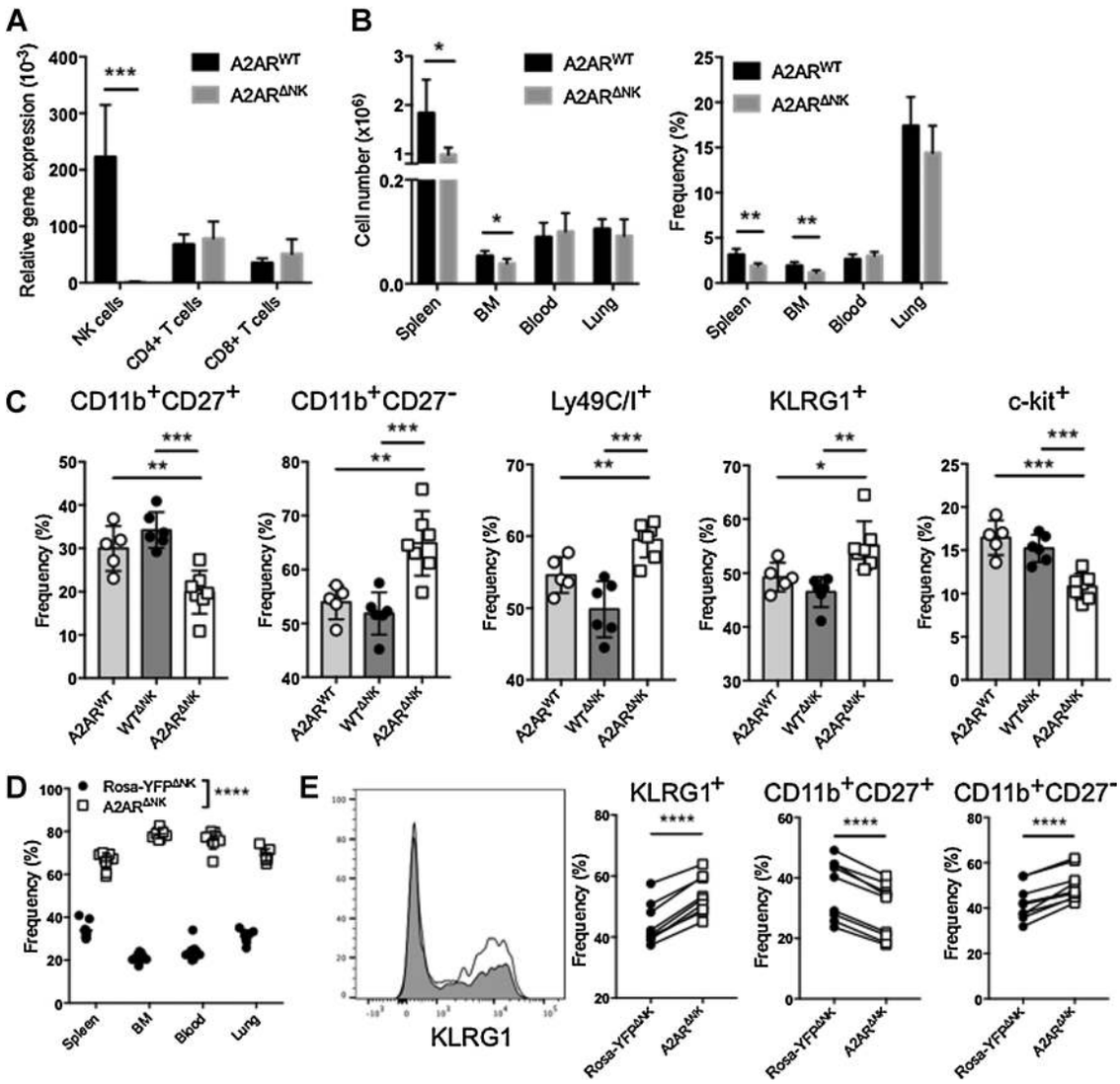

Figure 4.

NK-cell–specific A2AR-deletion maintains enhanced NK-cell maturation and proliferation. **A,** RNA from sorted splenic NK, $CD4^+$, and $CD8^+$ T cells was extracted and relative *ADORA2A* gene expression was measured by RT-PCR as compared with *HPRT* housekeeping gene from six biological replicates for each genotype *Ncr1*^{WT}A2AR$^{fl/fl}$ (A2AR^{WT}) and *Ncr1*^{iCre}A2AR$^{fl/fl}$ (A2AR$^{\Delta NK}$). **B,** Frequency and enumeration of NK cells (TCRβ$^-$NK1.1$^+$NKp46$^+$ of CD45.2$^+$ viable cells) from A2AR^{WT} or A2AR$^{\Delta NK}$ mice in the indicated organs (spleen, BM, blood, lung). **C,** Maturation markers including CD11b and CD27, Ly49C/I$^+$, KLRG1$^+$, and c-kit$^+$ were assessed for alteration in *Ncr1*^{iCre}A2AR$^{WT/WT}$ (WT$^{\Delta NK}$), *Ncr1*^{WT}A2AR$^{fl/fl}$ (A2AR^{WT}), and *Ncr1*^{iCre}A2AR$^{fl/fl}$ (A2AR$^{\Delta NK}$). **D,** Competitive bone marrow chimeras at a 50:50 ratio of *Ncr1*^{iCre}R26R^{eYFP} (Rosa-YFP$^{\Delta NK}$) and *Ncr1*^{iCre}A2AR$^{fl/fl}$ (A2AR$^{\Delta NK}$) donor NK cells were injected into PTPRCA recipients. Proportions of reconstituted NK cells were assessed by flow cytometry after 14 weeks in the indicated organs (spleen, BM, blood, lung). Comparison of statistical significance between Rosa-YFP$^{\Delta NK}$ and A2AR$^{\Delta NK}$ reconstitution in each organ is shown. **E,** As in **D**, flow cytometric analysis of maturation markers KLRG1, and CD11b and CD27 expression from donor Rosa-YFP$^{\Delta NK}$ and A2AR$^{\Delta NK}$ NK cells were compared from the same recipient. Representative histogram comparing KLRG1 expression from A2AR$^{\Delta NK}$ (unshaded histogram) and Rosa-YFP$^{\Delta NK}$ (shaded histogram) NK cells from the same recipient mice. Results shown are from one representative experiment of five to seven mice per genotype as indicated (**B** and **C**) and two representative donor pairs reconstituting nine recipients (**D** and **E**). Data are presented as mean ± SD. *, $P < 0.05$; **, $P < 0.01$; ***, $P < 0.001$; ****, $P < 0.0001$ determined by unpaired *t* test (**A–D**) and paired *t* test (**E**) from donor NK cells isolated from a shared recipient.

express CD39. Notably, when we divided NK cells based on the expression of CD11b and CD27 maturation markers we identified increasing proportions of $CD39^+$ expressing NK cells with maturation (Fig. 6F). We then assessed whether CD39 was altered on A2AR-deficient NK cells, and found that the proportions of $CD39^+$ NK cells were significantly increased (Fig. 6G).

A2AR antagonism modulates proportions of $CD56^{dim}$ human NK cells

As adenosine signaling on mouse NK cells appears to modulate maturation and the expression of enzymes that impact adenosine production, we next looked at whether human NK cells were impacted by adenosine signaling. We first assessed

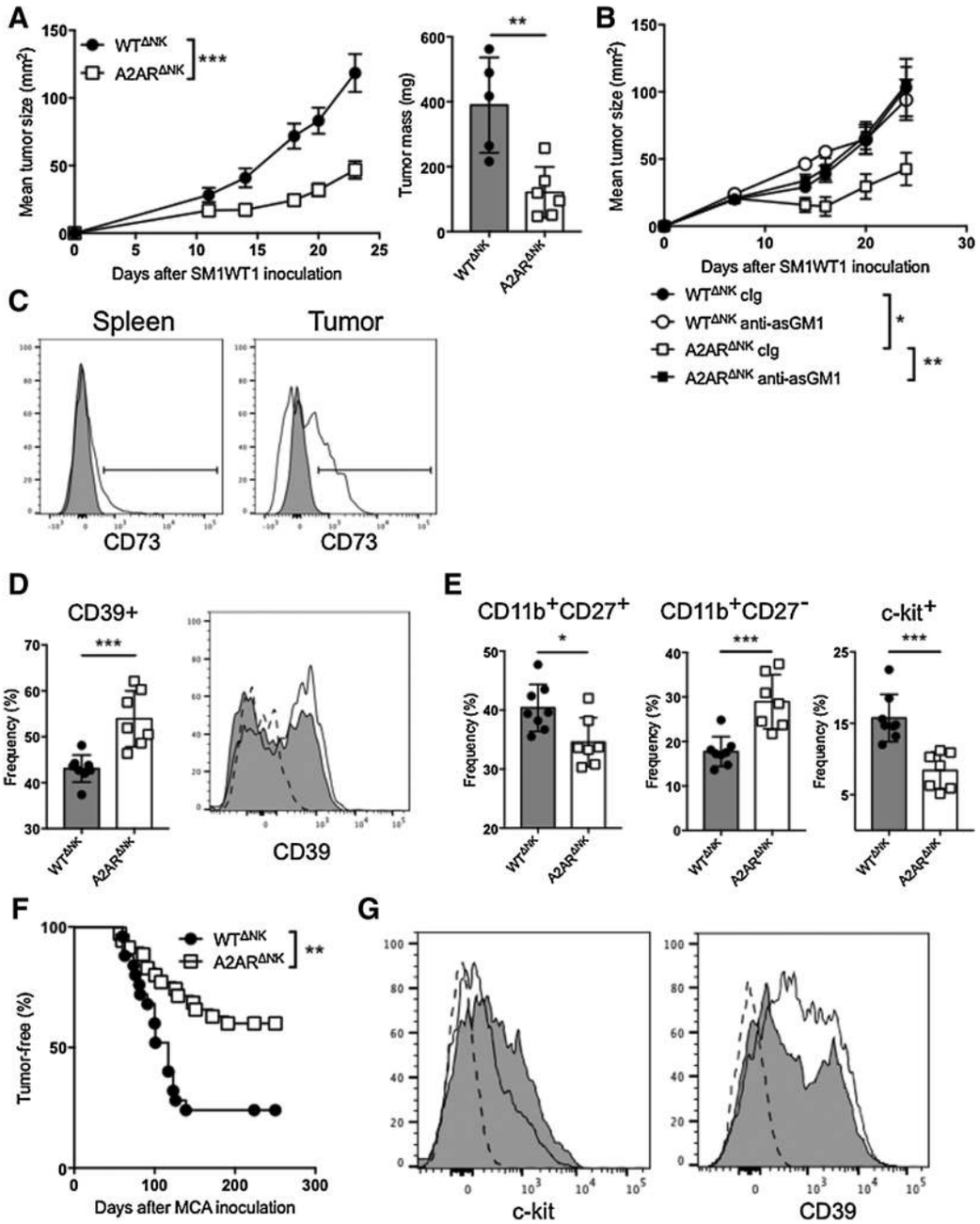

Figure 5.

A2AR-deficient NK cells improve tumor control. **A,** Growth of subcutaneous SM1WT1 tumor in *Ncr1*^{iCre}A2AR$^{WT/WT}$ (WT$^{\Delta NK}$) and *Ncr1*^{iCre}A2AR$^{fl/fl}$ (A2AR$^{\Delta NK}$) presented as mean ± SEM from five to six mice and statistical significance determined on day 23. Tumors were excised on day 24 and mass measured. **B,** SM1WT1 tumor growth in *Ncr1*^{iCre}A2AR$^{WT/WT}$ (WT$^{\Delta NK}$) and *Ncr1*^{iCre}A2AR$^{fl/fl}$ (A2AR$^{\Delta NK}$) mice depleted of NK cells by treatment with anti-asGM1 (100 μg i.p.) on day −1, 0, 7, and 14; tumor sizes are presented as means ± SEM from six to seven mice and statistical significance determined on day 24. **C,** Flow cytometric analysis of CD73 expression on NK cells isolated from spleen and tumor of C57BL/6 wild type mice at day 24 of SM1WT1 tumor growth. Representative histogram comparing CD73 expression (unshaded histogram) in tumor and spleen, isotype control (shaded histogram). **D,** Flow cytometric analysis and proportions of CD39-expressing NK cells isolated from SM1WT1 tumors at day 24 grown in seven to eight individual mice from the indicated genotypes. Representative histogram comparing CD39 expression from individual A2AR$^{\Delta NK}$ (unshaded histogram) and WT$^{\Delta NK}$ (shaded histogram) mice, isotype control (dashed line). **E,** Proportions of CD11b and CD27, and c-kit^{+} NK cells from day 24 SM1WT1 tumors grown in seven to eight individual mice from the indicated genotypes. **F,** Percentage of tumor-free *Ncr1*^{iCre}A2AR$^{WT/WT}$ (WT$^{\Delta NK}$) or *Ncr1*^{iCre}A2AR$^{fl/fl}$ (A2AR$^{\Delta NK}$) following inoculation with MCA. **G,** Representative histogram comparing c-kit and CD39 expression from endpoint tumors (greater than 100 mm^2) harvested on the same day from A2AR$^{\Delta NK}$ mice (unshaded histogram) and WT$^{\Delta NK}$ (shaded histogram) mice, isotype control (dashed line). Results shown are from one representative experiment (**A**, **C–E**, and **G**), one experiment (**B**), and two pooled experiments of 25–35 mice (**F**). Data are presented as mean ± SD unless otherwise indicated. **, $P < 0.01$; ***, $P < 0.001$ determined by unpaired *t* test (**A**, **C**, and **D**) and log-rank (Mantel–Cox) test (**E**).

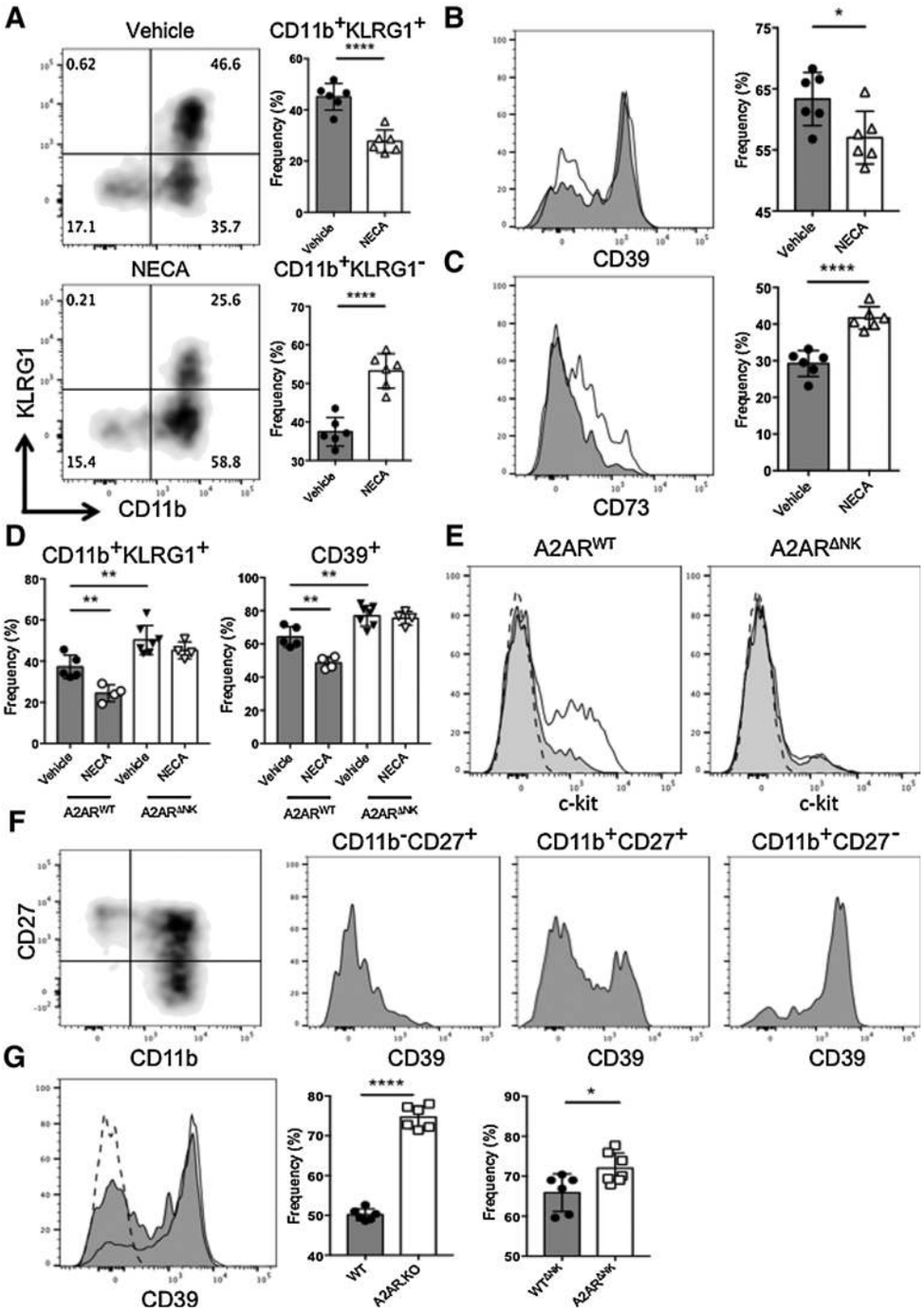

Figure 6.

Adenosine decreases NK-cell maturation and increases CD73 expression. **A,** C57BL/6 WT mice were treated with vehicle (DMSO) or NECA (0.05 mg/kg) injected intraperitoneally for 7 days. Flow cytometric analysis and proportions of NK-cell maturation subsets based on CD11b and KLRG1 expression in the spleen. **B** and **C,** As above in **A**, flow cytometric analysis and proportions of (**B**) CD39 and (**C**) CD73 expression on splenic NK cells. Representative histograms comparing NECA-treated (unshaded histogram) and vehicle-treated (shaded histogram) mice. **D,** $A2AR^{WT}$ and $A2AR^{\Delta NK}$ mice were treated with NECA (0.05 mg/kg) for 5 days. Proportions of CD11b and KLRG1 or $CD39^{+}$ splenic NK cells were determined by flow cytometry. **E,** As above in **D**, representative histograms comparing c-kit expression on splenic NK cells from $A2AR^{WT}$ or $A2AR^{\Delta NK}$ mice treated with NECA (unshaded histogram) or vehicle (shaded histogram), isotype control (dashed line). **F,** Representative histograms of CD39 expression on splenic NK-cell maturation subsets defined by CD11b and CD27. **G,** Flow cytometric analysis and proportions of $CD39^{+}$ expressing populations from splenic NK cells. Representative histogram comparing CD39 expression from individual A2AR.KO (unshaded histogram) and WT (shaded histogram) mice, isotype control (dashed line). Results shown are from one representative experiment of four to seven mice per group. Data are presented as mean ± SD. *, $P < 0.05$; **, $P < 0.01$; ****, $P < 0.0001$ determined by unpaired t test.

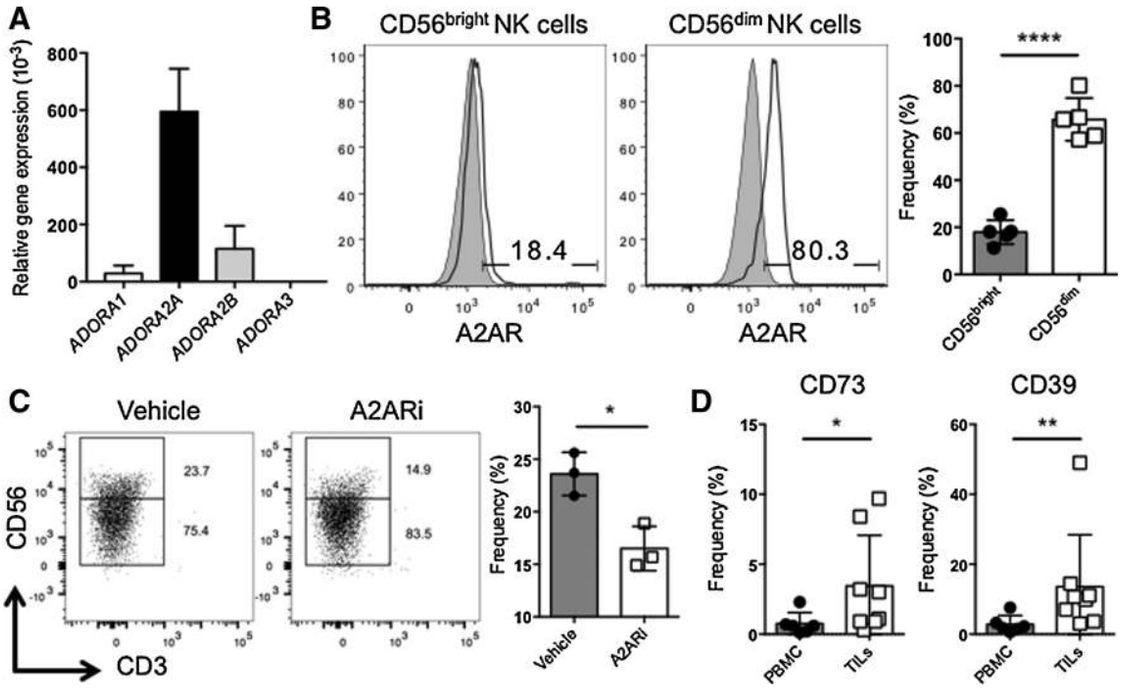

Figure 7.

A2AR inhibition reduces the proportion of CD56 bright NK cells. **A,** RNA from sorted human peripheral blood NK cells ($CD3^-CD56^+$) was extracted and relative adenosine receptor gene expression was measured compared with the *HPRT* housekeeping gene from three biological replicates. **B,** Flow cytometric analysis and proportions of A2AR expression in $CD56^{bright}$ and $CD56^{dim}$ NK cells was determined from five healthy subjects. Representative histogram comparing A2AR expression in $CD56^{bright}$ and $CD56^{dim}$ NK-cell subsets (unshaded histogram) compared with conventional T cells (shaded histogram). **C,** Sorted human NK cells were cultured for 6 days *in vitro* in IL2 (50 U/mL) in the presence of vehicle (DMSO) or A2ARi (SCH58261, 1 μmol/L) as specified. **D,** Proportions of CD73 and CD39 expression in NK cells ($CD3^-CD56^+$) assessed by flow cytometry from PBMCs and TILs isolated from GIST patients. Results shown are from one experiment of five subjects (**B**) and one representative experiment (**C**). Data are presented as mean ± SD. *, $P < 0.05$; **, $P < 0.01$; ****, $P < 0.0001$ determined by unpaired *t* test (**B** and **C**) and Mann–Whitney *U* test (**D**).

the gene expression of adenosine receptors present in NK cells ($CD3^-CD56^+$) isolated from human peripheral blood. The *ADORA2A* (A2AR) transcript was the predominant adenosine receptor expressed by human NK cells (Fig. 7A). Next, we assessed A2AR protein expression on human $CD56^{bright}$ and $CD56^{dim}$ NK cells isolated from the blood, compared to resting T cells. Notably, $CD56^{dim}$ NK cells displayed significantly higher levels of A2AR compared to both T cells and $CD56^{bright}$ NK-cell subsets (Fig. 7B). We then cultured human NK cells in the presence of IL2 alongside an A2AR inhibitor for 6 days. Interestingly, the proportion of $CD56^{bright}$ NK cells was reduced and a consequent increase in $CD56^{dim}$ NK cells apparent (Fig. 7C). In humans, $CD56^{bright}$ NK cells differentiate into $CD56^{dim}$ mature NK cells (19). Similar to the changes observed within mice, mature human NK cells accumulate following A2AR inhibition, indicative that eliminating this pathway further promotes the development of functionally mature NK cells. Finally, we assessed the expression of CD73 and CD39 on human NK cells infiltrating into GIST, for which NK cells have been shown to be an important predictor of therapeutic response (41, 42). Notably, CD73 and CD39 levels were significantly increased in GIST TILs comparatively to PBMCs isolated from GIST patients (Fig. 7D). This indicates that the adenosinergic pathway may be active to suppress NK-cell surveillance in cancer patients.

Discussion

Adenosine is emerging as a prominent immunotherapeutic target for use alone or as a combinatorial partner to front-line immune checkpoint blockade in the treatment of cancer. Due to the broad distribution of A2AR across multiple cell subsets (2), careful consideration of the therapeutic effects of A2AR antagonism on each cell type is required. In this study, we showed that global and conditional deletion of the A2AR on NK cells modulated NK-cell maturation at homeostasis, post-reconstitution, and within the tumor microenvironment. A2AR-deficient NK cells, particularly terminally mature $CD11b^+CD27^-$ NK cells, were also afforded a proliferative advantage. Importantly, although tumor-derived A2AR-deficient NK cells display enhanced maturation, they also provided protection against tumor development.

Clinical interest in NK-cell–based cancer immunotherapies has increased due to recognition of their active role in tumor immunosurveillance. Transfer of autologous or allogeneic NK cells as well as targeting immunosuppressive receptors and metabolites that impede NK-cell activation and tumor cell killing are currently being investigated (15, 43). Transferred NK cells require co-administration of cytokines (such as IL2 or IL15) to support expansion (44). However, IL2 also drives polarization of T regulatory cells, which produce soluble factors (including adenosine) that suppress NK-cell activity (45). A2AR antagonism may

promote the proliferation of functionally mature NK cells, without expansion of T regulatory cells. In addition, A2AR antagonism also facilitates improved infiltration of NK cells into solid tumor microenvironments and promotes expression of the cytolytic granule granzyme B (4, 37, 46). Often, adoptively-transferred NK cells persist within the circulation, however, their cytotoxic capacity is limited in patients, due to an unknown mechanism (47). Adenosine is a potent inhibitor of NK-cell cytotoxicity and cytokine production (4, 12, 13, 48). Furthermore, NK cells were critical for the therapeutic efficacy of respiratory hyperoxia treatment, which is also A2AR-dependent (49). Similarly, hypoxia enhances adenosine production, dampens NK-cell cyolytic activity and expression of essential activating receptors including NKG2D (50). Downregulation of NKG2D is apparent on NK cells isolated from patients following autologous NK-cell transfer (47), suggesting this suppressive mechanism may contribute to their ineffectual antitumor activity. Therefore, A2AR antagonism may potentiate the therapeutic efficacy of NK-cell–based therapeutic regimens.

Alongside direct enhancement of NK-cell function by genetically or therapeutically targeting the A2AR, limiting A2AR adenosine signaling on other cell subsets also indirectly promotes a favorable tumor microenvironment for NK-cell activity. Compared to A2AR-deficient NK cells, myeloid-specific A2AR deletion also provides improved tumor control and facilitates NK-cell activation by indirect mechanisms (7). In the absence of A2AR signaling, tumor-derived myeloid cells display reduced production of immunosuppressive IL10, leading to enhanced infiltration and antitumor activity of $CD8^+$ T cells and NK cells (7). In contrast, conditional A2AR deletion activates T cells, but in some instances, can also promote tumor growth by inhibiting T-cell maintenance and memory specifically within the tumor microenvironment (46). However, these effects may be tumor and dose dependent as in some tumor models global A2AR deletion, siRNA-induced reduction of the A2AR on T cells and therapeutic competitive receptor antagonism have been shown to demonstrate antitumor efficacy by T-cell–dependent mechanisms (3, 6, 37, 51). Furthermore, blockade of A2AR adenosine signaling inhibits T regulatory cell polarization, limiting T regulatory cell-mediated immunosuppression (9). Exploring therapeutic options that target A2AR signaling irreversibly in NK and myeloid cells, and partially on T cells may provide the greatest therapeutic protection.

Certain tumor types express high levels of CD39 and CD73, with tumor-derived adenosine able to markedly reduce NK-cell–mediated killing capacity (52). In this study, we showed that both the tumor microenvironment and exogenous adenosine enhanced NK cell expression of CD73, providing a potential self-intrinsic regulatory mechanism. Although CD73 expression on human NK cells isolated from peripheral blood is limited, it is increased in the presence of immunosuppressive mesenchymal stem cells (48). Similarly, TGFβ signaling in splenic NK cells enhanced CD73 expression (53). Others and we identified that ILC1s predominantly express CD73 in comparison to cNK cells (53). Furthermore, ILC1s and terminally mature NK cells highly express CD39, indicating that the adenosinergic pathway may be particularly active in regulating these cell types. Previously, CD39 expression on NK cells has been associated to co-regulation by T-BET and ZEB2 transcription factors during alternate stages of NK-cell maturation (24). We showed that A2AR-deficient NK cells heighten CD39 expression at homeostasis and in the tumor; however, whether this is a consequence of inferior adenosine signaling or solely a marker of NK-cell maturation has yet to be determined.

A2AR antagonism promoted the accumulation of human highly cytotoxic $CD56^{dim}$ NK cells *in vitro*. Notably, the transcriptional profile of A2AR-deficient $CD11b^+CD27^-$ NK cells resembled the differential expression of key molecules (such as *CXCR3*, *CX3CR1*, *IL18R*, and *KIT*) preferentially expressed on $CD56^{dim}$ compared to $CD56^{bright}$ human NK cells (54, 55). Previously, KIT expressing NK cells, induced by IL18 signaling, have been shown to be detrimental to tumor control (38). A2AR-deficient terminally mature NK cells displayed decreased *IL18R1* and *KIT* gene expression. Correspondingly, reduced proportions of KIT^+ NK cells were identified within the tumor microenvironment and in response to exogenous adenosine stimulus. Therefore, ablated A2AR adenosine signaling improves the quality and antitumor activity of NK cells infiltrating into the tumor microenvironment.

In summary, adenosine restricts NK-cell function and immune protection against tumor development. A2AR-engagement provides a checkpoint that negatively regulates the development of functionally mature NK cells. Because of the clinical use and excellent safety profiles of A2AR antagonists, targeting A2AR adenosine signaling in conjuction with NK-cell–based immunotherapies should be interrogated to determine whether this combinatorial strategy improves therapeutic efficacy.

Disclosure of Potential Conflicts of Interest

E. Vivier reports receiving a commercial research grant from Innate-Pharma and is also a consultant/advisory board member for Innate-Pharma. M.J. Smyth reports receiving a commercial research grant from Bristol Myers Squibb, Tizona Therapeutics, Aduro Biotech, and Corvus Pharmaceuticals, and is also a consultant/advisory board member for Tizona Therapeutics. No potential conflicts of interest were disclosed by the other authors.

Authors' Contributions

Conception and design: A. Young, F. Souza-Fonseca Guimaraes, M.J. Smyth
Development of methodology: A. Young, S.F. Ngiow, K.A. Stannard, M.A. Degli-Esposti, J. Linden, F. Souza-Fonseca Guimaraes
Acquisition of data (provided animals, acquired and managed patients, provided facilities, etc.): A. Young, S.F. Ngiow, Y. Gao, D.S. Barkauskas, M. Messaoudene, G. Lin, J.D. Coudert, K.A. Stannard, L. Zitvogel, M.A. Degli-Esposti, E. Vivier, N.D. Huntington, F. Souza-Fonseca Guimaraes
Analysis and interpretation of data (e.g., statistical analysis, biostatistics, computational analysis): A. Young, S.F. Ngiow, Y. Gao, A.M. Patch, M. Messaoudene, G. Lin, J.D. Coudert, N. Waddell, F. Souza-Fonseca Guimaraes, M.J. Smyth
Writing, review, and/or revision of the manuscript: A. Young, S.F. Ngiow, Y. Gao, A.M. Patch, J. Linden, F. Souza-Fonseca Guimaraes, M.J. Smyth
Administrative, technical, or material support (i.e., reporting or organizing data, constructing databases): A. Young
Study supervision: A. Young, J. Linden, F. Souza-Fonseca Guimaraes, M.J. Smyth

Acknowledgments

The authors wish to thank Stefano Mangiola, Marit Inngjerdingen, Ludovic Martinet, Dipti Vijayan, and Stephen Blake for their helpful discussions and critical review of the manuscript. We thank Yuan Ji Day (Chang Gung University, Tauyuan, Taiwan) for creating the A2AR floxed mice. We also thank Liam Town and Kate Elder for maintaining the mice used in this study and the QIMR Berghofer animal facility and flow cytometry facilities for their assistance. A.Young was supported by a Cancer Council Queensland Ph.D. fellowship. M.J. Smyth was supported by a National Health and Medical Research Council of Australia (NHMRC) Senior Research Fellowship (1078671) and Project Grant (1120887), a Susan G. Komen Program Grant

(IIR12221504), and a Cancer Research Institute Clinical Strategy Team Grant. J. Linden was supported by a grant from the National Institutes of Health (R01 HL111969). S.F. Ngiow was supported by an NHMRC C.J. Martin Fellowship (1111469). F.S.F. Guimaraes was supported by a NHMRC Early Career Fellowship (1088703), a National Breast Cancer Foundation (NBCF) Fellowship (PF-15-008), and grant #1120725 awarded through the Priority-driven Collaborative Cancer Research Scheme and funded by Cure Cancer Australia with the assistance of Cancer Australia. N.D. Huntington is a recipient of a NH&MRC Project Grant, Melanoma Research Grant from the Harry J Lloyd Charitable Trust, and a Cancer Research Institute Clinical and Laboratory Integration Program (CLIP) grant.

The costs of publication of this article were defrayed in part by the payment of page charges. This article must therefore be hereby marked *advertisement* in accordance with 18 U.S.C. Section 1734 solely to indicate this fact.

Received September 14, 2017; revised October 31, 2017; accepted December 6, 2017; published OnlineFirst December 11, 2017.

References

1. Ohta A, Sitkovsky M. Role of G-protein-coupled adenosine receptors in downregulation of inflammation and protection from tissue damage. Nature 2001;414:916–20.
2. Young A, Mittal D, Stagg J, Smyth MJ. Targeting cancer-derived adenosine: new therapeutic approaches. Cancer Discov 2014;4:879–88.
3. Ohta A, Gorelik E, Prasad SJ, Ronchese F, Lukashev D, Wong MK, et al. A2A adenosine receptor protects tumors from antitumor T cells. Proc Natl Acad Sci U S A 2006;103:13132–7.
4. Beavis PA, Divisekera U, Paget C, Chow MT, John LB, Devaud C, et al. Blockade of A2A receptors potently suppresses the metastasis of CD73+ tumors. Proc Natl Acad Sci U S A 2013;110:14711–6.
5. Hatfield SM, Kjaergaard J, Lukashev D, Belikoff B, Schreiber TH, Sethumadhavan S, et al. Systemic oxygenation weakens the hypoxia and hypoxia inducible factor 1alpha-dependent and extracellular adenosine-mediated tumor protection. J Mol Med 2014;92:1283–92.
6. Young A, Ngiow SF, Barkauskas DS, Sult E, Hay C, Blake SJ, et al. Co-inhibition of CD73 and A2AR Adenosine signaling improves anti-tumor immune responses. Cancer Cell 2016;30:391–403.
7. Cekic C, Day YJ, Sag D, Linden J. Myeloid expression of adenosine A2A receptor suppresses T and NK cell responses in the solid tumor microenvironment. Cancer Res 2014;74:7250–9.
8. Csoka B, Himer L, Selmeczy Z, Vizi ES, Pacher P, Ledent C, et al. Adenosine A2A receptor activation inhibits T helper 1 and T helper 2 cell development and effector function. FASEB J 2008;22:3491–9.
9. Ohta A, Kini R, Subramanian M, Madasu M, Sitkovsky M. The development and immunosuppressive functions of CD4(+) CD25(+) FoxP3(+) regulatory T cells are under influence of the adenosine-A2A adenosine receptor pathway. Front Immunol 2012;3:190. doi: 10.3389/fimmu.2012.00190.
10. Linnemann C, Schildberg FA, Schurich A, Diehl L, Hegenbarth SI, Endl E, et al. Adenosine regulates CD8 T-cell priming by inhibition of membrane-proximal T-cell receptor signalling. Immunology 2009;128: e728–e37.
11. Cekic C, Sag D, Day YJ, Linden J. Extracellular adenosine regulates naive T cell development and peripheral maintenance. J Exp Med 2013;210: 2693–706.
12. Lokshin A, Raskovalova T, Huang X, Zacharia LC, Jackson EK, Gorelik E. Adenosine-mediated inhibition of the cytotoxic activity and cytokine production by activated natural killer cells. Cancer Res 2006;66:7758–65.
13. Raskovalova T, Huang X, Sitkovsky M, Zacharia LC, Jackson EK, Gorelik E. Gs protein-coupled adenosine receptor signaling and lytic function of activated NK cells. J Immunol 2005;175:4383–91.
14. Jiao Y, Huntington ND, Belz GT, Seillet C. Type 1 innate lymphoid cell biology: lessons learnt from natural killer cells. Front Immunol 2016; 7:426. doi: 10.3389/fimmu.2016.00426.
15. Guillerey C, Huntington ND, Smyth MJ. Targeting natural killer cells in cancer immunotherapy. Nat Immunol 2016;17:1025–36.
16. Hayakawa Y, Smyth MJ. CD27 dissects mature NK cells into two subsets with distinct responsiveness and migratory capacity. J Immunol 2006; 176:1517–24.
17. Huntington ND, Tabarias H, Fairfax K, Brady J, Hayakawa Y, Degli-Esposti MA, et al. NK cell maturation and peripheral homeostasis is associated with KLRG1 up-regulation. J Immunol 2007;178:4764–70.
18. Martinet L, Ferrari De Andrade L, Guillerey C, Lee JS, Liu J, Souza-Fonseca-Guimaraes F, et al. DNAM-1 expression marks an alternative program of NK cell maturation. Cell Rep 2015;11:85–97.
19. Caligiuri MA. Human natural killer cells. Blood 2008;112:461–9.
20. Sathe P, Delconte RB, Souza-Fonseca-Guimaraes F, Seillet C, Chopin M, Vandenberg CJ, et al. Innate immunodeficiency following genetic ablation of Mcl1 in natural killer cells. Nat Commun 2014;5:4539. doi: 10.1038/ncomms5539.
21. Delconte RB, Shi W, Sathe P, Ushiki T, Seillet C, Minnich M, et al. The Helix-Loop-Helix Protein ID2 governs NK cell fate by tuning their sensitivity to interleukin-15. Immunity 2016;44:103–15.
22. Luevano M, Madrigal A, Saudemont A. Transcription factors involved in the regulation of natural killer cell development and function: an update. Front Immunol 2012;3:319. doi: 10.3389/fimmu.2012.00319.
23. Holmes ML, Huntington ND, Thong RP, Brady J, Hayakawa Y, Andoniou CE, et al. Peripheral natural killer cell maturation depends on the transcription factor Aiolos. EMBO J 2014;33:2721–34.
24. van Helden MJ, Goossens S, Daussy C, Mathieu AL, Faure F, Marcais A, et al. Terminal NK cell maturation is controlled by concerted actions of T-bet and Zeb2 and is essential for melanoma rejection. J Exp Med 2015;212: 2015–25.
25. Deng Y, Kerdiles Y, Chu J, Yuan S, Wang Y, Chen X, et al. Transcription factor Foxo1 is a negative regulator of natural killer cell maturation and function. Immunity 2015;42:457–70.
26. Chan CJ, Martinet L, Gilfillan S, Souza-Fonseca-Guimaraes F, Chow MT, Town L, et al. The receptors CD96 and CD226 oppose each other in the regulation of natural killer cell functions. Nat Immunol 2014;15:431–8.
27. Narni-Mancinelli E, Chaix J, Fenis A, Kerdiles YM, Yessaad N, Reynders A, et al. Fate mapping analysis of lymphoid cells expressing the NKp46 cell surface receptor. Proc Natl Acad Sci U S A 2011;108:18324–9.
28. Knight DA, Ngiow SF, Li M, Parmenter T, Mok S, Cass A, et al. Host immunity contributes to the anti-melanoma activity of BRAF inhibitors. J Clin Invest 2013;123:1371–81.
29. Koya RC, Mok S, Otte N, Blacketor KJ, Comin-Anduix B, Tumeh PC, et al. BRAF inhibitor vemurafenib improves the antitumor activity of adoptive cell immunotherapy. Cancer Res 2012;72:3928–37.
30. Rosin DL, Robeva A, Woodard RL, Guyenet PG, Linden J. Immunohistochemical localization of adenosine A2A receptors in the rat central nervous system. J Comp Neurol 1998;401:163–86.
31. Gao Y, Souza-Fonseca-Guimaraes F, Bald T, Ng SS, Young A, Ngiow SF, et al. Tumor immunoevasion by the conversion of effector NK cells into type 1 innate lymphoid cells. Nat Immunol 2017;18:1004–15.
32. Dobin A, Davis CA, Schlesinger F, Drenkow J, Zaleski C, Jha S, et al. STAR: ultrafast universal RNA-seq aligner. Bioinformatics 2013;29:15–21.
33. Li B, Dewey CN. RSEM: accurate transcript quantification from RNA-Seq data with or without a reference genome. BMC Bioinform 2011; 12:323. doi: 10.1186/1471-2105-12-323.
34. Robinson MD, McCarthy DJ, Smyth GK. edgeR: a Bioconductor package for differential expression analysis of digital gene expression data. Bioinformatics 2010;26:139–40.
35. Delconte RB, Kolesnik TB, Dagley LF, Rautela J, Shi W, Putz EM, et al. CIS is a potent checkpoint in NK cell-mediated tumor immunity. Nat Immunol 2016;17:816–24.
36. Revilla IDR, Bilic I, Vilagos B, Tagoh H, Ebert A, Tamir IM, et al. The B-cell identity factor Pax5 regulates distinct transcriptional programmes in early and late B lymphopoiesis. EMBO J 2012;31:3130–46.
37. Mittal D, Young A, Stannard K, Yong M, Teng MW, Allard B, et al. Antimetastatic effects of blocking PD-1 and the adenosine A2A receptor. Cancer Res 2014;74:3652–8.
38. Terme M, Ullrich E, Aymeric L, Meinhardt K, Coudert JD, Desbois M, et al. Cancer-induced immunosuppression: IL-18-elicited immunoablative NK cells. Cancer Res 2012;72:2757–67.

39. Smyth MJ, Crowe NY, Godfrey DI. NK cells and NKT cells collaborate in host protection from methylcholanthrene-induced fibrosarcoma. Int Immunol 2001;13:459–63.
40. Eini H, Frishman V, Yulzari R, Kachko L, Lewis EC, Chaimovitz C, et al. Caffeine promotes anti-tumor immune response during tumor initiation: Involvement of the adenosine A2A receptor. Biochem Pharmacol 2015;98: 110–8.
41. Chaput N, Flament C, Locher C, Desbois M, Rey A, Rusakiewicz S, et al. Phase I clinical trial combining imatinib mesylate and IL-2: HLA-DR+ NK cell levels correlate with disease outcome. Oncoimmunology 2013;2: e23080. doi: 10.4161/onci.23080.
42. Menard C, Blay JY, Borg C, Michiels S, Ghiringhelli F, Robert C, et al. Natural killer cell IFN-gamma levels predict long-term survival with imatinib mesylate therapy in gastrointestinal stromal tumor-bearing patients. Cancer Res 2009;69:3563–9.
43. Krasnova Y, Putz EM, Smyth MJ, Souza-Fonseca-Guimaraes F. Bench to bedside: NK cells and control of metastasis. Clin Immunol 2017;177:50–59.
44. Vitale M, Cantoni C, Pietra G, Mingari MC, Moretta L. Effect of tumor cells and tumor microenvironment on NK-cell function. Eur J Immunol 2014; 44:1582–92.
45. Deaglio S, Dwyer KM, Gao W, Friedman D, Usheva A, Erat A, et al. Adenosine generation catalyzed by CD39 and CD73 expressed on regulatory T cells mediates immune suppression. J Exp Med 2007;204:1257–65.
46. Cekic C, Linden J. Adenosine A2A receptors intrinsically regulate CD8+ T cells in the tumor microenvironment. Cancer Res 2014;74:7239–49.
47. Parkhurst MR, Riley JP, Dudley ME, Rosenberg SA. Adoptive transfer of autologous natural killer cells leads to high levels of circulating natural killer cells but does not mediate tumor regression. Clin Cancer Res 2011;17:6287–97.
48. Chatterjee D, Tufa DM, Baehre H, Hass R, Schmidt RE, Jacobs R. Natural killer cells acquire CD73 expression upon exposure to mesenchymal stem cells. Blood 2014;123:594–5.
49. Hatfield SM, Kjaergaard J, Lukashev D, Schreiber TH, Belikoff B, Abbott R, et al. Immunological mechanisms of the antitumor effects of supplemental oxygenation. Sci Transl Med 2015;7:277ra30.
50. Balsamo M, Manzini C, Pietra G, Raggi F, Blengio F, Mingari MC, et al. Hypoxia downregulates the expression of activating receptors involved in NK-cell-mediated target cell killing without affecting ADCC. Eur J Immunol 2013;43:2756–64.
51. Waickman AT, Alme A, Senaldi L, Zarek PE, Horton M, Powell JD. Enhancement of tumor immunotherapy by deletion of the A2A adenosine receptor. Cancer Immunol Immunother 2012;61: 917–26.
52. Hausler SF, Montalban del Barrio I, Strohschein J, Chandran PA, Engel JB, Honig A, et al. Ectonucleotidases CD39 and CD73 on OvCA cells are potent adenosine-generating enzymes responsible for adenosine receptor 2A-dependent suppression of T cell function and NK cell cytotoxicity. Cancer Immunol Immunother 2011;60:1405–18.
53. Cortez VS, Cervantes-Barragan L, Robinette ML, Bando JK, Wang Y, Geiger TL, et al. Transforming growth factor-beta signaling guides the differentiation of innate lymphoid cells in salivary glands. Immunity 2016;44: 1127–39.
54. Cooper MA, Fehniger TA, Caligiuri MA. The biology of human natural killer-cell subsets. Trends Immunol 2001;22:633–40.
55. Campbell JJ, Qin S, Unutmaz D, Soler D, Murphy KE, Hodge MR, et al. Unique subpopulations of CD56+ NK and NK-T peripheral blood lymphocytes identified by chemokine receptor expression repertoire. J Immunol 2001;166:6477–82.